Earth and Planetary Science Letters 516 (2019) 49–55

Contents lists available at ScienceDirect

Earth and Planetary Science Letters

www.elsevier.com/locate/epsl

# Evaluation of ice-stream model sensitivities for parameter estimation

Richard B. Alley [a,*], Wenjie Li [b], Byron R. Parizek [a,c], Fuqing Zhang [b,*]

[a] Department of Geosciences, and Earth and Environmental Systems Institute, The Pennsylvania State University, University Park, PA, USA
[b] Department of Meteorology, and Advanced Data Assimilation and Predictability Techniques Center, The Pennsylvania State University, University Park, PA, USA
[c] Mathematics and Geoscience, The Pennsylvania State University, DuBois, PA, USA

ARTICLE INFO

*Article history:*
Received 9 October 2018
Received in revised form 18 March 2019
Accepted 24 March 2019
Available online 9 April 2019
Editor: W.B. McKinnon

*Keywords:*
glacier flow
parameter estimation
model sensitivity
data assimilation
ice stream
data uncertainty

ABSTRACT

Large-ensemble perturbed-parameter forward ice-flow modeling can provide useful insights to uncertainties in inversions for basal drag or other ice-flow parameters. Inversion and data assimilation provide estimates of poorly known parameters that are essential for accurate prognostic modeling. Because ice flow depends on many such parameters with their associated uncertainties, which may interact in nonlinear ways, full uncertainty assessment for parameter estimates is challenging. With rising computational power, it is increasingly practicable to explore co-dependencies and sensitivities. Here, we use a well-characterized higher-order flowline model configured for a well-lubricated ("shelfy") ice stream to run large ensembles, perturbing the magnitude and spatial pattern of basal drag, basal topography, and input flux. We find for steady state that ice-stream velocity and thickness along the entire domain are especially correlated to drag at the downstream end, but with greater local correlation during transients. The modeled effects of basal topographic perturbations on velocity and ice thickness are primarily local. Perturbations of input ice fluxes interact with the others in interesting ways. These insights point to the value of inversions informed by concentrated observations during forced transients such as lake-drainage events, accumulation-rate fluctuations or ice-shelf losses, and to the care needed when interpreting local results of some inversions for basal-drag parameters.



## 1. Introduction

Sea-level rise remains one of the most consequential, but uncertain, aspects of climate change (e.g., Oppenheimer and Alley, 2016). Ice sheets hold by far the largest reservoir of potential sea-level rise (e.g., Lemke et al., 2007), so uncertainties regarding ice-sheet behavior are especially important. Changing snowfall and melt can affect ice-sheet mass balance and thus sea level, but the potential for large and rapid sea-level change arises especially from possible changes in flow of or calving from the fast-moving ice streams that drain the large inland reservoirs (e.g., Joughin et al., 2012; DeConto and Pollard, 2016). Models of fast-moving ice thus are of considerable importance in assessments of impacts of changing climate.

In common with many other geophysical models, ice-flow models rely heavily on parameterizations. For example, ice deformation may occur by dislocation glide or climb, grain boundary sliding, migration of point defects, and other processes (e.g., Alley, 1992; Goldsby and Kohlstedt, 2001), leading to changes in grain size, c-axis fabric, and defect character and abundance that feed back on the deformation. Much is understood about many of these processes, but few ice-flow models seek to simulate them explicitly, instead replacing this complexity with a representative power-law dependence of strain rate on stress.

The numerical values of a suite of parameters then must be specified in some fashion, including a power, a prefactor, and perhaps an enhancement factor (which may be a scalar or a tensor) and an activation energy. All of these may be functions of measurable quantities, varying with position, temperature, age of ice, accumulated deformation, applied stress or other controls. Estimation of functions may be done based on laboratory data addressing fundamental ice physics or ice deformation. Again, in common with other geophysical modeling, parameter estimation is increasingly done through data assimilation or inversion techniques, using the observed characteristics of an ice stream or streams to estimate the parameters and quantify their uncertainties.

A formal argument can be made (Nielsen-Gammon et al., 2010) that the total number of parameters applicable to a geophysical model is essentially unbounded; with more observations, one could estimate more parameters in ways that would improve model fits and might improve the ability of models to project future changes. Observed data are always limited, however, and thus inadequate to estimate all the parameters that a process-based sci-

* Corresponding authors.
*E-mail addresses:* rba6@psu.edu (R.B. Alley), fuz4@psu.edu (F. Zhang).

https://doi.org/10.1016/j.epsl.2019.03.035
0012-821X/

entist could suggest. Hence, a subset of parameters must be chosen for optimization, and the errors associated with the choice as well as the optimization should be considered before assimilating data for parameter estimation.

As discussed by Nielsen-Gammon et al. (2010) addressing meteorological models, parameters should be chosen that are identifiable, distinguishable and preferably monotonic. Identifiable parameters are those that detectably affect observable aspects of the behavior of the model. Individual impacts that are monotonic functions of parameter values allow accurate parameter estimation with quantifiable uncertainties, in particular when using a best linear unbiased estimator such as the ensemble Kalman filter (EnKF) (Evensen, 1994; Houtekamer and Zhang, 2016). And, the effects of distinguishable impacts can be isolated and optimized.

Based on the ensemble sensitivity analysis of a large number of perturbed-parameter experiments in Nielsen-Gammon et al. (2010), successful parameter estimation experiments with the EnKF assimilating real-data observations were conducted that led to improved parameterization of atmospheric boundary processes and consequently improved atmospheric state estimations (Hu et al., 2010). Similarly, based on systematic sensitivity analysis of a large ensemble of perturbed-parameter forward-model experiments in Shi et al. (2014), the EnKF assimilation of multivariate, high temporal resolution, in-situ measurements from a local watershed can efficiently and effectively optimize key parameters in physically-based land surface hydrologic models (Shi et al., 2015).

Here, we conduct an ensemble sensitivity analysis on a subset of parameters that we consider important in a simple but well-characterized higher-order ice-stream model (Parizek and Walker, 2010; Parizek et al., 2010, 2013). We focus on parameters that strongly affect flow and can be measured or estimated from measured quantities, including basal topography and friction, and input flux, varying thickness and input velocity separately or together. Following Nielsen-Gammon et al. (2010) and Shi et al. (2014), we report on a large suite of forward simulations varying these parameters within likely ranges, and we assess nonlinearities, interactions, and influence. These simulations produce insights described below, which we believe will prove useful in data assimilation going forward. In particular, we find strong reason to conduct ensembles of model runs across the uncertain parameters to accurately characterize total model uncertainties, and to focus data collection and data assimilation on transient systems to improve characterization of local conditions. Additional results are given in Li (2018).

## 2. Experimental design

Experiments are conducted for a reference ice stream using the 2-D PSU flowline model (Parizek and Walker, 2010; Parizek et al., 2010, 2013). This is a well-characterized finite-element model that has been applied in many ways (e.g., Parizek et al., 2010, 2013; Christianson et al., 2013; Applegate et al., 2015; Holschuh et al., 2017). It is run here in a higher-order flowband mode, configured to resemble a Siple Coast, West Antarctica ice stream (e.g., Bentley, 1987) without exactly matching any particular ice stream. Grid resolution is 500 m, reduced down to 50 m at domain boundaries for the momentum balance, with 35 vertically-stretching layers in the ice (∼30-m spacing, reduced to a few meters at the upper and lower boundaries for the momentum balance).

Flowband width is specified constant at 100 km, wide enough that side drag is not especially important. Initially, ice 1054-m thick flows into the 50-km-long region of interest at 228 m/yr. An otherwise gently sloping bed (deepening along flow with a slope of −0.003 from an upstream depth of −200 m) includes a single Gaussian topographic feature centered at 25 km along flow of extent (standard deviation of the Gaussian) 2 km along flow, which

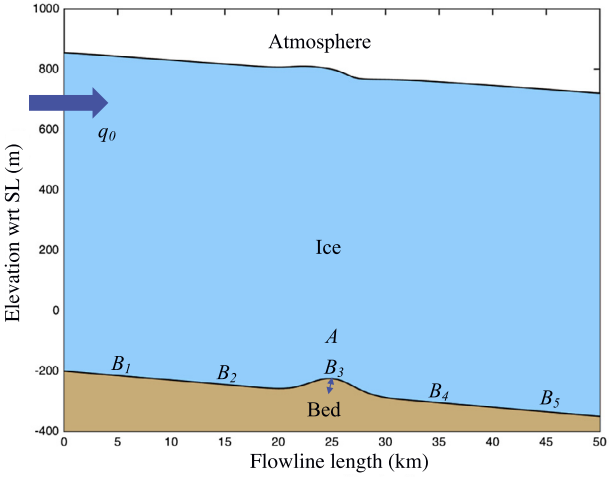


**Fig. 1.** Sketch of the ice-stream model, showing the topographic feature with amplitude A, and the different regions of bed friction $B_1$-$B_5$ from upstream to downstream.

is perturbed from the reference height A = 50 m for assessment of effects of basal topography (Fig. 1). The basal friction coefficient is perturbed from the reference value $B_{b\_o} = 1.3 \times 10^6$ Pa s$^{1/3}$ m$^{-1/3}$, providing a well-lubricated ice stream for which basal sliding dominates motion.

For each experiment, we start with steady-state conditions, perturb parameters instantly, and then run toward a new steady state for at least 100 yrs (some experiments are extended to 200 yrs, as indicated below). For each 0.5-km-long grid box along the ice stream, we calculate at 20-yr intervals (10-yr intervals in some cases) the ensemble correlation—the correlation between the perturbed model parameter(s) and the modeled thickness, and separately the modeled surface velocity, for the 51 members included in each ensemble. This ensemble size was chosen to be large enough to give statistically significant results without overly taxing computer resources.

The (near-steady) correlation values at the end of each experiment show the sensitivity of thickness and surface velocity to the poorly known parameters, of interest in assessing uncertainties in inversions and for informing decisions about observational campaigns to reduce uncertainties. The nonsteady values are also of interest, because significant natural perturbations can occur over timescales short compared to our 20-yr reporting interval. For example, drainage of subglacial lakes can redistribute basal drag on subannual timescales (e.g., Gray et al., 2005), evolution of basal topography has been observed over few-year timescales (e.g., Smith et al., 2007), and kinematic waves can affect flux and thickness rapidly (e.g., Nye, 1960).

We perturb this steady-state model as follows. For bottom terrain height (A), we perturb the amplitude from 0.5 to 1.5 of the control value in steps of 0.02 while maintaining the same extent along flow. For the basal friction coefficient $B_{bo}$, we perturb from 0.5 to 1.5 times the control value in steps of 0.02; this is applied either to the entire domain uniformly, or we divide the domain into five 10-km-long segments with B1 (upglacier) to B5 (downglacier) and apply perturbations to each, randomly chosen from the range used for $B_{bo}$. We also perturb input flux by 1% or 5%, or separately perturb the thickness or input velocity by 5%. Perturbation magnitudes were chosen to be large enough to provide significant changes, but to fall within the range of uncertainties that might occur in existing datasets. For experiments addressing particular parts of an extant ice sheet, perturbation magnitudes can be chosen based on the available data.

The various perturbations are modeled individually, or together with random perturbations of other parameters. The full suite of

**Table 1**
List of experiments.

| Expt # | A | B1 | B2 | B3 | B4 | B5 | Qflux | Qspeed | Qdepth |
|---|---|---|---|---|---|---|---|---|---|
| 1a | +/−50% | | | | | | | | |
| 1b | | +/−50% | = B1 | = B1 | = B1 | = B1 | | | |
| 1c | +/−50% | +/−50% | = B1 | = B1 | = B1 | = B1 | | | |
| 2 | | +/−50% | +/−50% | +/−50% | +/−50% | +/−50% | | | |
| 3 | +/−50% | +/−50% | +/−50% | +/−50% | +/−50% | +/−50% | | | |
| 4a | | +/−50% | +/−50% | +/−50% | +/−50% | +/−50% | +/−5% | | |
| 4b | | +/−50% | +/−50% | +/−50% | +/−50% | +/−50% | +/−1% | | |
| 5 | +/−50% | +/−50% | +/−50% | +/−50% | +/−50% | +/−50% | +/−5% | | |
| 6a | +/−50% | +/−50% | +/−50% | +/−50% | +/−50% | +/−50% | | +/−5% | |
| 6b | +/−50% | +/−50% | +/−50% | +/−50% | +/−50% | +/−50% | | | +/−5% |
| 6c | +/−50% | +/−50% | +/−50% | +/−50% | +/−50% | +/−50% | | +/−5% | +/−5% |

experiments discussed here is detailed in Table 1. Some of the experiments use ensembles that uniformly sample the parameter space (e.g., terrain height) whereas others provide a probabilistic sample from the parameter space. We conducted additional experiments, some of which are reported in Li (2018), to more fully explore the influence of parameter uncertainties.

## 3. Results

Here, we briefly review the main results of the experiments, presenting figures showing the more instructive ones and providing additional figures in the Supporting Material.

### 3.1. Experiments with basal friction coefficient independent of position

In Experiment 1a, we vary terrain height A. Results are shown in Fig. 2, in a form that will be followed for subsequent plots. Results for times 20, 40, 60, 80 and 100 yrs after the initial perturbation are color-coded. The left-hand panels show the spatial pattern of the correlation between the thickness (top row) and velocity (bottom row) for each time, and the corresponding standard deviations of the ice thickness (top) and surface velocity (bottom) are shown in the right panels.

A higher topographic bump causes additional form drag, leading to thicker ice upstream (hence positive correlation for $x < \sim$20 km) and slower velocity there (negative correlation) due to the constant influx boundary condition, with time-evolution downstream leading to thinner, faster ice there. Thickness and velocity are affected strongly over the bump itself, as shown by the large standard deviation there, with smaller effects upstream of the bump and very small effects downstream.

Uniform perturbation of the basal friction coefficient over the whole domain (Experiment 1b; Fig. S1a) generates strong correlations over the entire domain, with higher friction giving slower and thicker ice for all times. Effects on thickness are larger at the upstream end, as the input flux is held fixed, and steady state is not reached after 100 yrs.

The combined effects of perturbations of terrain height A chosen randomly from Experiment 1a and basal friction coefficient $B_{bo}$ chosen randomly from Experiment 1b are shown in Fig. S1b (Experiment 1c). The effects of both variables are clearly evident in correlations and standard deviations. For the magnitudes of perturbations applied here, the basal friction coefficient is more important (correlation magnitudes generally greater than 0.8 and nearly 1.0 except over the bump, compared to correlation magnitudes for terrain height of $<$0.2 except transiently over the bump).

### 3.2. Experiments with spatially variable basal friction coefficient

All subsequent experiments vary the basal friction coefficient within the same range as before, but, as described above, with five independent values chosen randomly from the same distribution as before, and applied to segments B1 from 0-10 km, ..., to B5 from 40-50 km along flow. For Experiment 2, all else is held constant except for the basal friction values (other parameters are varied in additional experiments described below). The results are shown in Figs. 3a and 3b. Consistent with the results described above for spatially uniform values, higher B correlates with slower, thicker ice. A perturbation has an important impact within its own segment and in all segments farther upglacier, with smaller influence downglacier. Correlations are largest for the downglacier-most segment B5, and smaller for all others.

The standard deviations show that thickness changes are largest upglacier, and velocity changes are largest downglacier. Changes in both thickness and velocity increase over time, as shown by the standard deviations in Figs. 3a and 3b, except for some initial decrease in velocity sensitivity, likely due to spin-up interactions with the fixed input flux.

Correlations also evolve over time as the influence of a segment spreads upglacier. This is especially true for the downglacier segment 5; its influence grows to dominate conditions in the whole domain, with a coupled decrease in the importance of the other segments.

Experiment 3 was then run, combining perturbations of B1-B5 with perturbations of terrain height A, again with all perturbations randomly chosen from the ranges previously specified, and an ensemble of 51 runs generated. These Experiment 3 runs are extended to 200 yrs.

As shown in Fig. S2a-c, the effect of adding perturbations in A to those in B1-B5 is similar to the effect of adding perturbations in A to $B_{bo}$. The correlation structures are recognizably similar to those for which A is held constant; for the perturbation magnitudes chosen, B is more important than A. The topographic perturbations A are most important in the flowline segment containing the topographic feature. The topographic perturbations reduce the correlation coefficients between downglacier friction (B5) and upglacier velocity and thickness (segments 1 and 2), especially for short times while those correlations are increasing toward their steady values.

By the end of the 200-yr runs, the correlation coefficients are nearly steady (Figs. S2a-b), and are shown in Fig. 4. The standard deviations (Fig. S2c), however, continue to evolve, showing that the thickness and velocity have not yet fully reached steady state. Fig. 4 shows the local importance of the topography, and the dominant influence of the friction coefficient in the downglacier-most segment on the entire flowline.

### 3.3. Experiments adding variable ice input to domain

Experiments 4-6 repeat Experiments 2-3, but with the addition of variable ice input at the upglacier end. In Experiments 4-5, the input flux is varied, with perturbation values randomly selected from a Gaussian distribution with zero mean and standard deviation of 0.05 (i.e., 5% uncertainty in the default ice input

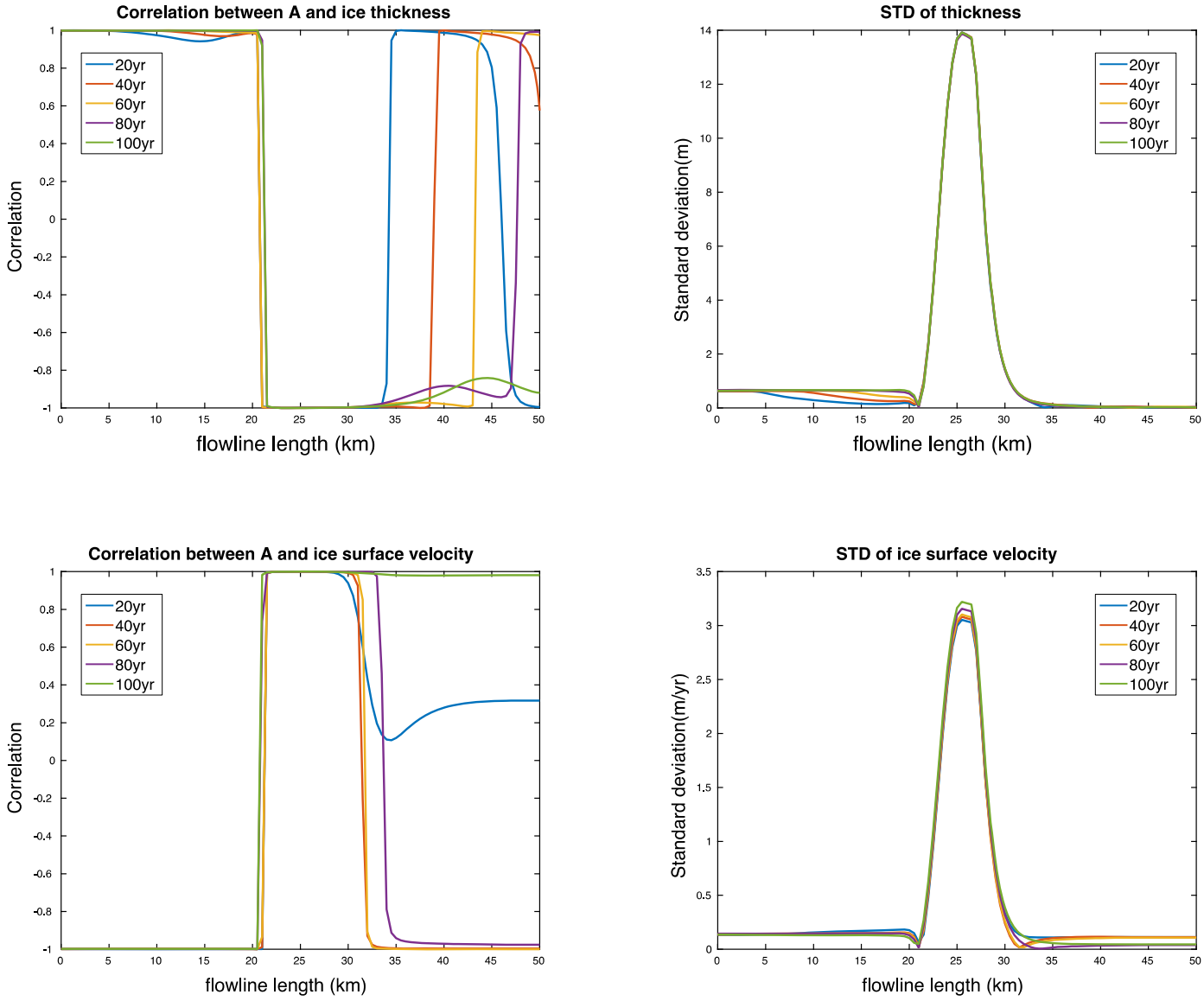


**Fig. 2.** Results of Experiment 1a, varying terrain height A. Shown are the correlation between A and ice thickness (upper left) and surface velocity $u$ (lower left), and standard deviations of thickness (upper right) and velocity (lower right).

flux) for Experiments 4a and 5, and zero mean and standard deviation of 0.01 (i.e., 1% of the default input flux) for Experiment 4b, with the random choices of other perturbed variables from their ranges used in Experiments 2-3. In these Experiments 4-5, the model dynamically partitions the variable flux into changes in velocity and thickness. In Experiment 6, the input velocity and thickness are varied separately, with perturbation values randomly selected from a Gaussian distribution with zero mean and standard deviation of 0.05, applied to input velocity in Experiment 6a, to thickness along the whole domain in 6b, and to both in 6c (see below). Experiments 4a and 4b otherwise repeat Experiment 2 in maintaining fixed topography (A) and randomly choosing spatially variable basal friction coefficients (B1-B5). Experiments 5 and 6 repeat Experiment 3 in randomly choosing perturbations in both basal topography (A) and friction (B1-B5). Experiments are summarized in Table 1.

The results of Experiment 4a are shown in Figs. S3a-c. The model solves the momentum balance before the mass balance, and with the highly lubricated bed, this primarily partitions the input-flux perturbations into velocity perturbations rather than thickness perturbations; thus, the model produces little correlation between input flux and thickness along the domain, but strong positive correlation between input flux and velocity. The correlations with B1-B5, and their time-evolution, maintain the same form as in Experiment 2, with little change in magnitude for thickness but reduced magnitude for velocity, reflecting the strong velocity correlation to input flux. Reducing the perturbations on input flux to 1% in Experiment 4b (Figs. S4a-c) preserves the same basic patterns, but reduces the strength of correlation between input flux and velocities along the domain, shifting the results towards those from Experiment 2 with no variation of input flux.

The results of Experiment 5, repeating Experiment 3 with the addition of input-flux perturbations, are shown in Figs. S5a-c. As before, introduction of input-flux perturbations primarily affects velocity, and otherwise the results from Experiment 3 are repeated.

Finally, in Experiments 6a-6c, we perturb thickness and inlet velocity, together with basal topography and drag. Thickness is perturbed along the whole flowband to simulate domain-wide uncertainty in surface and basal elevations. Results are shown for 5% perturbations on inlet velocity (S6a-c) and separately on thickness (S7a-c), and on both inlet velocity and thickness (S8a-c). Faster ice flow at the upglacier end produces faster ice flow along the whole

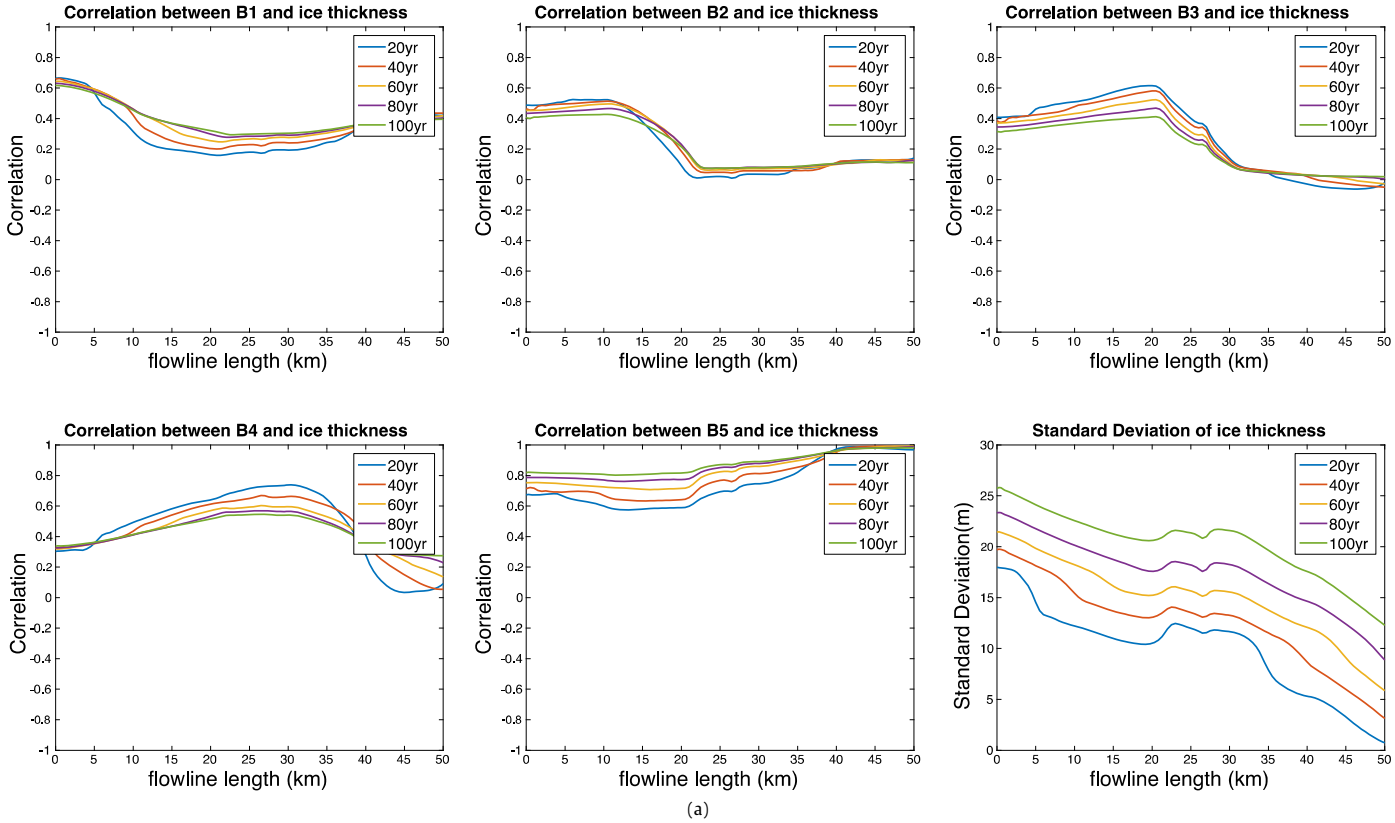


(a)

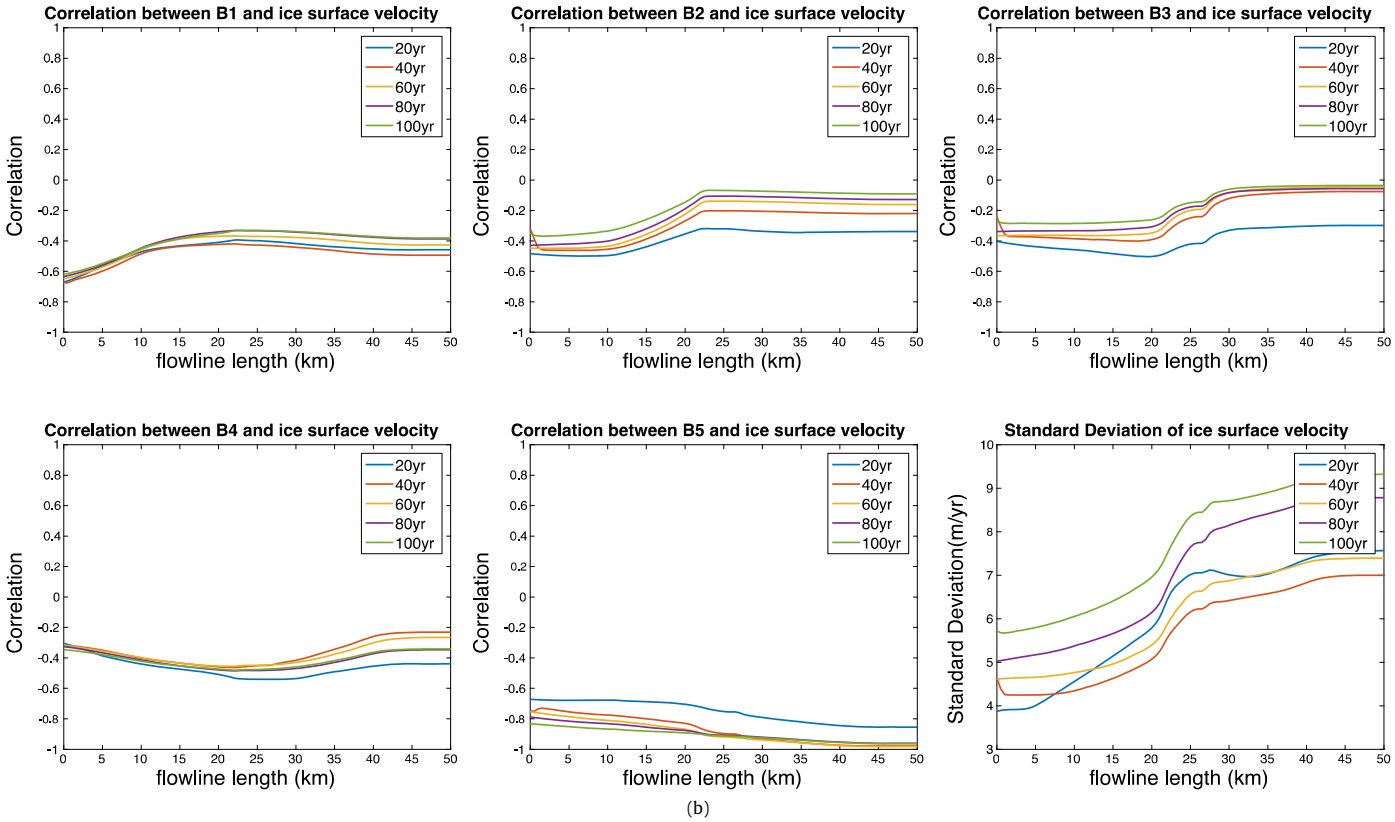


(b)

**Fig. 3.** (a) Results of Experiment 2, independently varying friction B1, . . . , B5. Shown are the correlation between B for each section and ice thickness, as indicated, together with the standard deviation of thickness (lower right). (b) As in Fig. 3a, but showing the correlation to surface velocity $u$, and the standard deviation of the surface velocity.

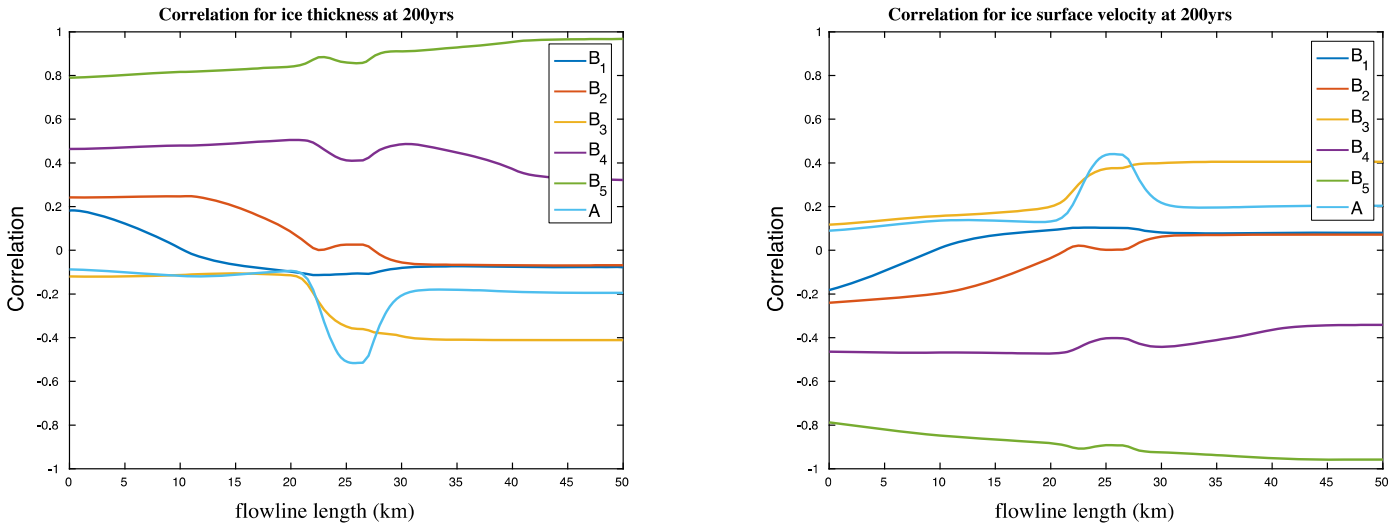


**Fig. 4.** Results of Experiment 3, independently perturbing topography and friction in different segments. Shown, at the end of 200 yrs, are correlation between either thickness (left) or surface velocity (right), and terrain height A and friction coefficients B1, . . . , B5.

domain, transmitted rapidly downstream in this well-lubricated system. Large changes in thickness or inlet velocity dominate the correlations, but the structure of the remaining, small correlations to friction and topography remains similar to results with fixed inlet thickness and velocity as shown above.

## 4. Discussion

Use of data to invert for uncertain model parameters is of great and increasing value in glaciological modeling (e.g., MacAyeal et al., 1995; Vieli and Payne, 2003; Joughin et al., 2004, 2006; Vieli et al., 2006; Goldberg and Sergienko, 2011; Larour et al., 2012; Morlighem et al., 2013; Zhao et al., 2018; and many more), including time-evolving as well as "snapshot" data (e.g., Walker et al., 2012; Larour et al., 2014). Most commonly, the data used include ice-surface velocities and elevations, which usually are available with greater accuracy and higher spatial resolution than other relevant fields. Bed elevations are often included, providing ice thickness. Other data (deformation of internal layers, bed character, borehole deformation, c-axis fabrics, ice temperature) have been used, or may be used in the future. Parameters estimated may include basal friction or the basal flow law more generally, as these are needed for time-stepping. Such estimates may be affected by uncertainties in ice flux from internal deformation, as well as by uncertainties in the thickness and velocity data themselves.

Following, e.g., Nielsen-Gammon et al. (2010), we conducted a suite of forward ice-stream simulations, generating ensembles for perturbations of key parameters including basal friction, bed topography, and upglacier velocity and ice flux, and we have calculated the correlations of these parameters to surface velocity and ice thickness. The results of similar studies applied to actual data could be used to optimize field programs seeking to reduce uncertainties. Because even such improved data will still include uncertainties, the techniques discussed here are also useful to estimate errors that these uncertainties introduce to inversions, allowing improved estimates of uncertainties in ensemble projections.

In addition to addressing such uncertainties, the runs here provide some insights to ice-stream response to time-varying conditions. Input flux may be perturbed significantly by kinematic waves propagating downglacier (e.g., Nye, 1960). Basal lubrication evolves in response to numerous processes, some of which remain poorly characterized. For example, waves may develop in the basal water system as well as in the ice (e.g., Kyrke-Smith et al., 2014), with subglacial outburst floods providing an extreme example (e.g., Winberry et al., 2009). Unconsolidated beds can evolve rapidly, with Smith et al. (2007) having documented sediment erosion at 1 $\mathrm{m\,yr^{-1}}$ over 6 yrs and deposition of a drumlin 10 m high and 100 m across over 7 yrs beneath an Antarctic ice stream, and Motyka et al. (2006) showing widespread bed-elevation changes including erosion at 3.9 $\mathrm{m\,yr^{-1}}$ over 14 yrs beneath Taku Glacier, Alaska. The potential for rapid changes is particularly large in the grounding zone of marine-ending glaciers, where numerous processes interact (e.g., Horgan et al., 2013). One can use site-specific knowledge to assess likely perturbations and their magnitude, and then apply ensemble simulations to assess their importance to the ice stream.

Our runs highlight several potentially interesting avenues for further research. These include:

→ The perturbations of basal topography we simulated have significant local effects on thickness, but much smaller effects beyond the topographic disturbance either upglacier or downglacier, and relatively smaller effects on flow velocity;

→ Perturbations of basal friction as well as topography initially have strong local effects; but

→ With increasing time, the effects of perturbations in basal friction extend upglacier, and as steady state is approached, the "buttressing" effects of perturbations beneath the downglacier-most segment grow to exceed the effects of local perturbations along the entire domain, strongly focusing attention on grounding-zone processes;

→ Large uncertainties in input flux can obscure other controls on thickness and velocity.

We emphasize that we analyze results from one control setup of one model, which has not been exactly matched to any real ice-sheet setting. Our study thus does not directly address any past, ongoing, or future data-assimilation projects. We believe, nonetheless, that adding correlation analyses such as this one to future projects can improve the fidelity of those results. Incorporating data for nonsteady systems can be especially useful.

## 5. Conclusions

Uncertainties in inversions for basal drag or other ice-flow parameters can be estimated usefully with large-ensemble perturbed-parameter forward ice-flow modeling. This technique also can provide insight to the influence of time-varying forcing on ice-stream flow. Broader application of this technique thus could be used to improve prognostic models of ice-sheet behavior.

We find that drag at the downstream end is especially important in controlling steady-state motion along the full length of an ice stream, but that local conditions are more important during transients. This in turn recommends focusing field observations in the grounding zone, and using time-varying conditions to estimate conditions upstream.

## Acknowledgements

We thank the Advanced Data Assimilation and Predictability Techniques Center of The Pennsylvania State University for support. Partial funding was provided by the National Science Foundation through AGS-1338832 (RBA, BRP), AGS-1712290 (FZ), PLR-1443190 (BRP), and NSF-NERC-OPP-1738934 (RBA, BRP), by NASA under grant NNX15AH84G (BRP), and by the Heising-Simons Foundation under grant 2018-0769 (RBA, BRP). Metadata and selected data from Li (2018) that underlie this paper are archived at http://www.datacommons.psu.edu/commonswizard/MetadataDisplay.aspx?Dataset=6215.

## Appendix A. Supplementary material

Supplementary material related to this article can be found online at https://doi.org/10.1016/j.epsl.2019.03.035.

## References

Alley, R., 1992. Flow-law hypotheses for ice-sheet modeling. J. Glaciol. 38 (129), 245–256. https://doi.org/10.3189/S0022143000003658.

Applegate, P.J., Parizek, B.R., Nicholas, R.E., Alley, R.B., Keller, K., 2015. Increasing temperature forcing reduces the Greenland Ice Sheet's response time scale. Clim. Dyn. 45, 2001–2011. https://doi.org/10.1007/s00382-014-2451-7.

Bentley, C.R., 1987. Antarctic ice streams: a review. J. Geophys. Res. 92 (B9), 8843–8858. https://doi.org/10.1029/JB092iB09p08843.

Christianson, K., Parizek, B.R., Alley, R.B., Horgan, H.J., Jacobel, R.W., Anandakrishnan, S., Keisling, B.A., Craig, B.D., Muto, A., 2013. Ice sheet grounding zone stabilization due to till compaction. Geophys. Res. Lett. 40, 1–6. https://doi.org/10.1002/2013GL057447.

DeConto, R.M., Pollard, D., 2016. Contribution of Antarctica to past and future sea-level rise. Nature 531, 591–597. https://doi.org/10.1038/nature17145.

Evensen, G., 1994. Sequential data assimilation with a nonlinear quasi-geostrophic model using Monte Carlo methods to forecast error statistics. J. Geophys. Res. 99 (C5), 10143–10162. https://doi.org/10.1029/94JC00572.

Goldberg, D.N., Sergienko, O.V., 2011. Data assimilation using a hybrid ice flow model. Cryosphere 5 (2). https://doi.org/10.5194/tc-5-315-2011.

Goldsby, D.L., Kohlstedt, D.L., 2001. Superplastic deformation of ice: experimental observations. J. Geophys. Res., Solid Earth 106 (B6), 11017–11030. https://doi.org/10.1029/2000JB900336.

Gray, L., Joughin, I., Tulaczyk, S., Spikes, V.B., Bindschadler, R., Jezek, K., 2005. Evidence for subglacial water transport in the West Antarctic Ice Sheet through three-dimensional satellite radar interferometry. Geophys. Res. Lett. 32 (3), L03501. https://doi.org/10.1029/2004GL021387.

Holschuh, N., Parizek, B.R., Alley, R.B., Anandakrishnan, S., 2017. Decoding ice sheet behavior using englacial layer slopes. Geophys. Res. Lett. 44. https://doi.org/10.1002/2017/GL073417.

Horgan, H.J., Alley, R.B., Christianson, K., Jacobel, R.W., Anandakrishnan, S., Muto, A., Beem, L.H., Siegfried, M.R., 2013. Estuaries beneath ice sheets. Geology 41 (11), 1159–1162. https://doi.org/10.1130/G34654.1.

Houtekamer, P.L., Zhang, F., 2016. Review of the ensemble Kalman filter for atmospheric data assimilation. Mon. Weather Rev. 144, 4490–4530. https://doi.org/10.1175/MWR-D-15-0440.1.

Hu, X.-M., Zhang, F., Nielsen-Gammon, J.W., 2010. Ensemble-based simultaneous state and parameter estimation for treatment of mesoscale model error: a real-data study. Geophys. Res. Lett. 37, L08802. https://doi.org/10.1029/2010GL043017.

Joughin, I., MacAyeal, D.R., Tulaczyk, S., 2004. Basal shear stress on the Ross ice streams from control method inversions. J. Geophys. Res., Solid Earth 109, B09405. https://doi.org/10.1029/2003JB002960.

Joughin, I., Bamber, J.L., Scambos, T., Tulaczyk, S., Fahnestock, M., MacAyeal, D.R., 2006. Integrating satellite observations with modeling: basal shear stress of the Filchner-Ronne ice streams, Antarctica. Philos. Trans. R. Soc. A, Math. Phys. Eng. Sci. 364 (1844), 1795–1814. https://doi.org/10.1098/rsta.2006.1799.

Joughin, I., Alley, R.B., Holland, D.M., 2012. Ice-sheet response to oceanic forcing. Science 338, 1172–1176. https://doi.org/10.1126/science.1226481.

Kyrke-Smith, T.M., Katz, R.F., Fowler, A.C., 2014. Subglacial hydrology and the formation of ice streams. Proc. R. Soc. Lond., Ser. A 470, 20130494. https://doi.org/10.1098/rspa.2013.0494.

Larour, E., Seroussi, H., Morlighem, M., Rignot, E., 2012. Continental scale, high order, high spatial resolution, ice sheet modeling using the Ice Sheet System Model (ISSM). J. Geophys. Res., Earth Surf. 117 (F1). https://doi.org/10.1029/2011JF002140.

Larour, E., Utke, J., Csatho, B., Schenk, A., Seroussi, H., Morlighem, M., et al., 2014. Inferred basal friction and surface mass balance of the Northeast Greenland Ice Stream using data assimilation of ICESat (Ice Cloud and land Elevation Satellite) surface altimetry and ISSM (Ice Sheet System Model). Cryosphere 8 (6), 2335–2351. https://doi.org/10.5194/tc-8-2335-2014.

Lemke, P., Ren, J., Alley, R.B., Allison, I., Carrasco, J., Flato, G., Fujii, G., Kaser, Y., Mote, P., Thomas, R.H., Zhang, T., 2007. Observations: changes in snow, ice and frozen ground. In: Solomon, S., Qin, D., Manning, M., Chen, Z., Marquis, M., Averyt, K.B., Tignor, M., Miller, H.L. (Eds.), Climate Change 2007: The Physical Science Basis. Contribution of Working Group I to the Fourth Assessment Report of the Intergovernmental Panel on Climate Change. Cambridge University Press, Cambridge, UK, New York, NY, USA.

Li, Wenji, 2018. Ensemble Sensitivity Analysis of Ice Flow Simulations with Different Parametric Model Uncertainties. M.Sc. thesis. Meteorology, Pennsylvania State University, University Park, PA. 32 pp. https://etda.libraries.psu.edu/files/final_submissions/17978.

MacAyeal, D.R., Bindschadler, R.A., Scambos, T.A., 1995. Basal friction of ice stream E, West Antarctica. J. Glaciol. 41, 247–262. https://doi.org/10.3189/S0022143000016154.

Morlighem, M., Seroussi, H., Larour, E., Rignot, E., 2013. Inversion of basal friction in Antarctica using exact and incomplete adjoints of a higher-order model. J. Geophys. Res., Earth Surf. 118 (3), 1746–1753. https://doi.org/10.1002/jgrf.20125.

Motyka, R.J., Truffer, M., Kuriger, E.M., Bucki, A.K., 2006. Rapid erosion of soft sediments by tidewater glacier advance: Taku Glacier, Alaska, USA. Geophys. Res. Lett. 33, L24504. https://doi.org/10.1029/2006GL028467.

Nielsen-Gammon, J.W., Hu, Z.-M., Zhang, F., Pleim, J.E., 2010. Evaluation of planetary boundary layer scheme sensitivities for the purpose of parameter estimation. Mon. Weather Rev. 138, 3400–3417. https://doi.org/10.1175/2010MWR3292.1.

Nye, J.F., 1960. The response of glaciers and ice-sheets to seasonal and climatic changes. Proc. R. Soc. Ser. A 256 (1287), 559–584. https://doi.org/10.1098/rspa.1960.0127.

Oppenheimer, M., Alley, R.B., 2016. How high will the seas rise? Science 354 (6318), 1375–1377. https://doi.org/10.1126/science.aak9460.

Parizek, B.R., Alley, R.B., Dupont, T.K., Walker, R.T., Anandakrishnan, S., 2010. Effect of orbital-scale climate cycling and meltwater drainage on ice sheet grounding line migration. J. Geophys. Res. 115, F01011. https://doi.org/10.1029/2009JF001325.

Parizek, B.R., Walker, R.T., 2010. Implications of initial conditions and ice-ocean coupling on grounding-line evolution. Earth Planet. Sci. Lett. 300, 351–358. https://doi.org/10.1016/j.epsl.2010.10.016.

Parizek, B.R., Christianson, K., Anandakrishnan, S., Alley, R.B., Walker, R.T., Edwards, R.A., Wolfe, D.S., Bertini, G.T., Rinehart, S.K., Bindschadler, R.A., Nowicki, S.M.J., 2013. Dynamic (in)stability of Thwaites Glacier, West Antarctica. J. Geophys. Res., Earth Surf. 118, 1–18. https://doi.org/10.1002/jgrf.20044.

Shi, Y., Davis, K.J., Zhang, F., Duffy, C.J., 2014. Evaluation of the parameter sensitivities of a coupled land surface hydrologic model at a critical zone observatory. J. Hydrometeorol. 15, 279–299. https://doi.org/10.1175/JHM-D-12-0177.1.

Shi, Y., Davis, K.J., Zhang, F., Duffy, C.J., Yu, X., 2015. Parameter estimation of a physically-based land surface hydrologic model using an ensemble Kalman filter: a multivariate real-data experiment. Adv. Water Resour. 83, 421–427. https://doi.org/10.1016/j.advwatres.2015.06.009.

Smith, A.M., Murray, T., Nicholls, K.W., Makinson, K., Aoalgeirsdottir, G., Behar, A.E., Vaughan, D.G., 2007. Rapid erosion, drumlin formation, and changing hydrology beneath an Antarctic ice stream. Geology 35 (2), 127–130. https://doi.org/10.1103/G23036A.

Vieli, A., Payne, A.J., 2003. Application of control methods for modelling the flow of Pine Island Glacier, West Antarctica. Ann. Glaciol. 36, 197–204. https://doi.org/10.3189/172756403781816338.

Vieli, A., Payne, A.J., Du, Z., Shepherd, A., 2006. Numerical modelling and data assimilation of the Larsen B ice shelf, Antarctic Peninsula. Philos. Trans. R. Soc. A, Math. Phys. Eng. Sci. 365, 1815–1839. https://doi.org/10.1098/rsta.2006.1800.

Walker, R.T., Christianson, K., Parizek, B.R., Anandakrishnan, S., Alley, R.B., 2012. A viscoelastic flowline model applied to tidal forcing of Bindschadler Ice Stream, West Antarctica. Earth Planet. Sci. Lett. 319–320, 128–132. https://doi.org/10.1016/j.epsl.2011.12.019.

Winberry, J.P., Anandakrishnan, S., Alley, R.B., 2009. Seismic observations of transient subglacial water-flow beneath MacAyeal Ice Stream, West Antarctica. Geophys. Res. Lett. 36, L11502. https://doi.org/10.1029/2009GL037730.

Zhao, C., Gladstone, R.M., Warner, R.C., King, M.A., Zwinger, T., Morlighem, M., 2018. Basal friction of Fleming Glacier, Antarctica – part 1: sensitivity of inversion to temperature and bedrock uncertainty. Cryosphere 12, 2637–2652. https://doi.org/10.5194/tc-12-2637-2018.